Anisotropic UH model for soils based on a simple transformed stress method

Yangping Yao[1 *], Yu Tian[1] and Zhiwei Gao[2]

[1] School of Transportation Science and Engineering, Beihang University, Beijing, 100191, China

[2] School of Engineering, University of Glasgow, Glasgow, G12 8QQ, UK

Abstract

A simple method, called anisotropic transformed stress (ATS) method, is proposed to develop failure criteria and constitutive models for anisotropic soils. In this method, stress components in different directions are modified differently in order to reflect the effect of anisotropy. It includes two steps of mapping of stress. First, a modified stress tensor is introduced which is a symmetric multiplication of stress tensor and fabric tensor. In the modified stress space, anisotropic soils can be treated to be isotropic. Second, a transformed stress tensor is derived from the modified stress tensor for the convenience of developing anisotropic constitutive models to account for the effect of intermediate principal stress. By replacing the ordinary stress tensor with the transformed stress tensor directly, the Unified Hardening (UH) model is extended to model the anisotropic deformation of soils. Anisotropic Lade's criterion is adopted for shear yield and shear failure in the model. The form of the original model formulations remain unchanged and the model parameters are independent of the loading direction. Good agreement between the experimental results and predictions of the anisotropic UH model is observed.

Keywords: anisotropy; fabric of soils; modified stress tensor; transformed stress tensor; failure criterion; constitutive relation

1. Introduction

Soils exhibit different stress-strain behaviors and strength properties when loaded in different directions due to the existence of anisotropy. For instance, Ladd [1] studied the stress-strain behaviors of isotropically and anisotropically consolidated clays in triaxial compression tests. It was found that the anisotropic samples showed much higher stiffness, lower axial strain to failure and strain-softening although the samples were normally consolidated. Duncan and Seed [2] showed that, when an undisturbed clay sample was loaded in different directions, the maximum difference in undrained shear strength could reach up to 30%. Arthur and Menzies indicated that the inherent anisotropy could cause over 200% differences in the axial strains required to reach a given stress ratio [3], while the stress-induced anisotropy did not significantly influence the shear strength but caused a deviation between the principal axes of stress and strain increments [4-5]. A series of true triaxial tests on cross-anisotropic San Francisco Bay mud were conducted by Kirkgard and Lade [6]. It was indicated that the Lade's criterion overestimated the strengths when the major principal stress was parallel to the bedding plane. Lade and Abelev [7] investigated the stiffness anisotropy of

* Corresponding Arthur. Tel: 86-10-61716636. Email: ypyao@buaa.edu.cn.

Nevada sand by isotropic compression tests. The compression modulus along the direction of deposition was 7.0-7.5 times higher than the bulk modulus.

Such anisotropic mechanical behaviors have significant influence on the design of infrastructures built in/on soils. Without proper consideration of soil anisotropy, the associated geotechnical design could be either too dangerous or unnecessarily conservative [8-9]. It is thus desirable to develop failure criterion and constitutive model which can properly account for the effect of anisotropy on failure and deformation properties of soils. Hill [10] is among the first to propose an anisotropic failure criterion. Since this criterion is based on the von Mises criterion, it is not suitable for soils the behaviors of which are always pressure dependent. An effective way of modelling anisotropic soils is to introduce a fabric tensor, which describes the internal structural anisotropy of soils [11-13], into the existing failure criteria/constitutive models for isotropic soils. For instance, Oda and Nakayama [14] introduced extra items associated with the fabric tensor into the Drucker-Prager's yield function. Pietruszczak and Mroz [15-16] proposed a critical plane approach in which cohesion and friction angle were assumed to vary with the fabric. The critical plane, on which the ratio of shear and normal stresses reaches the maximum bearing capacity, was found to be the failure plane according to the Mohr-Coulomb criterion. This method has also been used to extend the Lade's failure criterion [17] and to model the anisotropic stress-strain relations of soils [18-19]. Li and Dafalias [20-21] and Gao *et al*. [22-23] proposed an anisotropic variable which is a scalar-valued joint invariant of stress tensor and fabric tensor. Soil properties like failure and dilatancy were assumed to vary with the anisotropic variable. In summary, all of these methods assume that soil parameters are dependent on the loading direction. If a general formula $f(\sigma_{ij})=k$ is used to represent the isotropic failure/yield criteria in which k denotes material constants, the methods above will change k to be functions of the stress tensor σ_{ij} and the fabric tensor F_{ij} so that anisotropic models can be developed as $f(\sigma_{ij})=k(\sigma_{ij},F_{ij})$. These methods are flexible but many parameters for modifying k are needed to fit the experimental data.

In this paper, to consider the effect of anisotropy on the mechanical behaviors of soils, the relative magnitudes of stress components in different directions, rather than the soil parameters, are modified according to the fabric anisotropy. The process and result of the stress modification are shown in Fig. 1. The ordinary stress tensor σ_{ij} is first modified to be a modified stress tensor $\overline{\sigma}_{ij}$ in order to account for the effect of anisotropy, then to be a transformed stress tensor $\widetilde{\sigma}_{ij}$ using the TS (transformed stress) method [24-26] to account for the effect of intermediate principal stress. The anisotropic constitutive models developed in this paper can be expressed as $f(\widetilde{\sigma}_{ij})=k$ in which k is still independent of the loading direction.

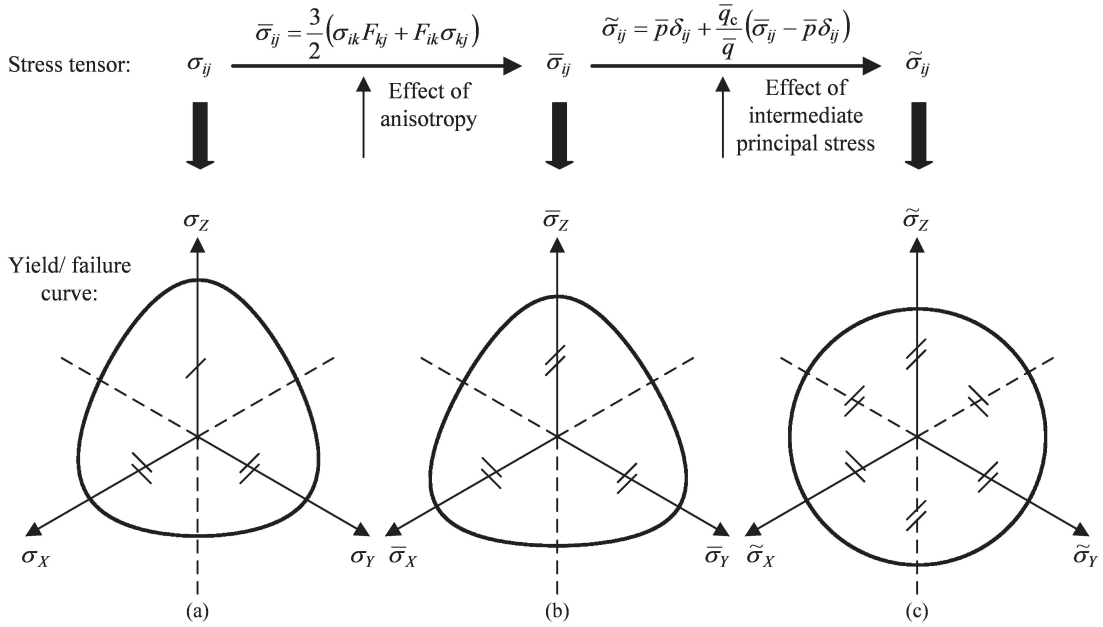

Fig. 1 Illustration of the ATS method

2. Fabric tensor

Micromechanical investigations have shown that fabric is the fundamental reason for the anisotropy of the mechanical behaviors of soils [27-28]. A fabric tensor is essential for constitutive modelling of anisotropic soils [29-30]. It quantifies the internal structure formed in soils, such as the spatial distribution of particles, voids or contact normals. Experimental tests show that the preferred orientation of soil particles would hardly change in monotonic loading even when considerable strain is reached [5, 12]. Therefore, a constant fabric tensor is adopted in this paper for convenience. Since the fabric of soils is typically cross-anisotropic, a practical fabric tensor F_{ij} is defined as below if the principal axes of the material fabric are aligned with the reference coordinates, with the *x*-*y* plane being the isotropic plane which is typically the bedding plane, and *z* the axis of anisotropy

$$F_{ij} = \begin{pmatrix} F_z & 0 & 0 \\ 0 & F_x & 0 \\ 0 & 0 & F_y \end{pmatrix} = \begin{pmatrix} \Delta & 0 & 0 \\ 0 & \frac{1}{2}(1-\Delta) & 0 \\ 0 & 0 & \frac{1}{2}(1-\Delta) \end{pmatrix} \tag{1}$$

where Δ is a positive variable related to the degree of anisotropy. For most soil deposits, the long axes of particles tend to be parallel to the *x*-*y* plane to remain stable, so that $\Delta < 1/3$. Smaller value of Δ indicates higher degree of anisotropy. When $\Delta = 1/3$, $F_{ij} = \delta_{ij}/3$ and the material is isotropic, where δ_{ij} (=1 for $i = j$ and 0 for $i \neq j$) is the Kronecker delta. The fabric tensor expressed in Eq. (1) must be subjected to orthogonal transformation if the reference frame changes or the material fabric plane is rotated.

3. Modified stress tensor

3.1 Basic formula

In order to model the mechanical behaviors of anisotropic soils, a convenient and effective way is to introduce the fabric tensor into the existing isotropic failure criteria and constitutive models. The most direct method is to use the fabric tensor to modify the strength or stiffness parameters in the models to be variables with the loading direction [15-23]. In this paper, fabric tensor is used to modify the stress. Based on the work of Tobita [31-32], a modified stress tensor is introduced as the product of F_{ij} and the ordinary stress tensor σ_{ij} as follows

$$\overline{\sigma}_{ij} = \frac{3}{2}\left(\sigma_{ik}F_{kj} + F_{ik}\sigma_{kj}\right) \tag{2}$$

It can be seen that $\overline{\sigma}_{ij}$ is symmetric and has the dimension of stress. The coefficient 3/2 makes $\overline{\sigma}_{ij} = \sigma_{ij}$ when the material is isotropic ($F_{ij} = \delta_{ij}/3$). This multiplication can be interpreted as that the relative magnitudes of components of σ_{ij} in different directions are modified differently according to the material fabric. After the modification, the anisotropic soil is equivalent to a 'virtual' isotropic soil in the modified stress space. That is to say, when loaded from different directions, the anisotropic soil exhibits similar strength or stiffness properties from the view of the modified stress. Therefore, the mechanical description for anisotropic soils becomes much easier to be developed.

3.2 Analysis in two special cases

Expressions of $\overline{\sigma}_{ij}$ under two special loading cases (Fig. 2) are shown here to analyse how $\overline{\sigma}_{ij}$ is capable of describing the anisotropy of soils and to facilitate the discussion in the subsequent sections.

Case 1: True triaxial loading with horizontal bedding plane

When the soil with horizontal bedding plane is subjected to true triaxial loading shown in Fig. 2a, $\overline{\sigma}_{ij}$ can be expressed

$$\overline{\sigma}_{ij} = \begin{pmatrix} 3\sigma_Z\Delta & 0 & 0 \\ 0 & \frac{3}{2}\sigma_X(1-\Delta) & 0 \\ 0 & 0 & \frac{3}{2}\sigma_Y(1-\Delta) \end{pmatrix} \tag{3a}$$

where σ_Z, σ_X and σ_Y represent principal stresses in the physical space (Z, X, Y), respectively. Since $\Delta < 1/3$, it can be seen from Eq. (3a) that $\overline{\sigma}_Z < \sigma_Z$, $\overline{\sigma}_X > \sigma_X$ and $\overline{\sigma}_Y > \sigma_Y$ ($\overline{\sigma}_Z$, $\overline{\sigma}_X$ and $\overline{\sigma}_Y$ are principal values of $\overline{\sigma}_{ij}$, respectively). Some properties of anisotropic soils can be explained by $\overline{\sigma}_{ij}$.

If $\sigma_Z = \sigma_X = \sigma_Y$, one will get $\overline{\sigma}_Z < \overline{\sigma}_X = \overline{\sigma}_Y$, which means that the stress state in the modified stress space is anisotropic although isotropic compression is carried on in fact. Therefore, $\overline{\sigma}_{ij}$ can be

used to predict the anisotropic deformations in isotropic compression tests [7].

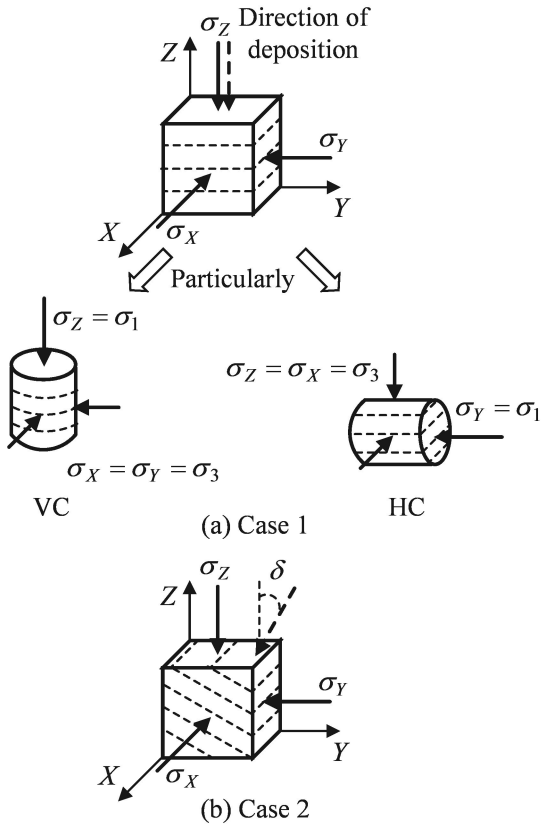

Fig. 2 True triaxial loading condition with (a) horizontal bedding plane and (b) inclined bedding plane

In this study, the conventional triaxial compression with the major principal stress being parallel to the direction of deposition ($\sigma_Z > \sigma_X = \sigma_Y$) is termed VC loading and the triaxial compression with the major principal stress being perpendicular to the direction of deposition ($\sigma_Z = \sigma_X < \sigma_Y$) is termed HC loading (Fig. 2a). In VC and HC loading, even if identical major and minor principal stresses are applied, the modified stresses are different since the stress modification is related to the direction. Therefore, anisotropy is revealed from the difference.

Case 2: True triaxial loading with inclined bedding plane

When the bedding plane is rotated around the *X*-axis as shown in Fig. 2b, orthogonal transformation for fabric tensor is needed when calculating $\overline{\sigma}_{ij}$ because the principal axes of the fabric tensor (z,x,y) do not coincide with the reference frame (Z,X,Y). Then $\overline{\sigma}_{ij}$ in (Z,X,Y) can be expressed as

$$\overline{\sigma}_{ij} = \frac{3}{8}\begin{pmatrix} 2\left[(1+\Delta)-(1-3\Delta)\cos 2\delta\right]\sigma_Z & 0 & (1-3\Delta)(\sigma_Z+\sigma_Y)\sin 2\delta \\ 0 & 4(1-\Delta)\sigma_X & 0 \\ (1-3\Delta)(\sigma_Z+\sigma_Y)\sin 2\delta & 0 & 2\left[(1+\Delta)+(1-3\Delta)\cos 2\delta\right]\sigma_Y \end{pmatrix} \quad (3b)$$

where δ is the angle between the vertical direction and direction of deposition. Note that there are shear stress components in $\overline{\sigma}_{ij}$ although only normal stresses are applied. Thus, sample distortion will be predicted in this case if $\overline{\sigma}_{ij}$ is used to calculate soil deformation. Again, this is supported by experimental observations [33-34].

It can be concluded from above that $\overline{\sigma}_{ij}$ provides a new manner to reflect the effect of anisotropy. Since anisotropic soils have been equivalent to isotropic soils in the modified stress space, the existing failure criteria such as the Lade's criterion [35], SMP criterion [36] or generalized non-linear strength criterion [37] can be extended to be anisotropic failure criteria by replacing σ_{ij} with $\overline{\sigma}_{ij}$. However, it is not suitable to introduce $\overline{\sigma}_{ij}$ directly into constitutive models such as the Cam-clay model [38-39]. Because the Cam-clay model was originally established under triaxial compression condition. It will bring in error if the Cam-clay model expressed by $\overline{\sigma}_{ij}$ is used to model the stress-strain relation of anisotropic soils without a proper consideration of the effect of intermediate principal stress. It is necessary to point out that the stress state is generally three-dimensional in geotechnical engineering. And what's more, even if triaxial compression loading is carried on, the stress state in the modified stress space will become true triaxial state. For example, in HC loading, one can get $\overline{\sigma}_Z < \overline{\sigma}_X < \overline{\sigma}_Y$ according to Eq. (3a). And even shear stress components will appear if the bedding plane is inclined (see Eq. (3b)). Therefore, the stress modification makes it more urgent to extend constitutive models to account for the effect of intermediate principal stress.

4. Transformed stress tensor

There are many methods to generalize constitutive models from the triaxial compression stress state to the 3D stress state, such as using a shape function of Lode's angle [40-41]. These methods have been discussed in Ref. [26]. In this paper, TS method [24-26] is used. In order to achieve the generalization, failure criteria, such as the Lade's criterion, are adopted for shear yield and shear failure of soils in the constitutive models in TS method. However, since the yield/failure curve in the deviatoric plane is irregular according to these criteria, they cannot be combined with constitutive models conveniently. TS method adopts a mapping of stress to consider the effect of intermediate principal stress, just like the stress modification to consider the effect of anisotropy. It projects the irregular yield/failure curve to its circumcircle by a mapping from σ_{ij} to the transformed stress tensor $\widetilde{\sigma}_{ij}$. In the transformed stress space, the shape of the yield surfaces in different meridian planes are adopted to be the same with that in the triaxial compression meridian plane. Therefore, constitutive models can be readily generalized to the true triaxial state in the transformed stress space, and then back to the ordinary stress space, the effect of intermediate principal stress can be reflected.

Referring to the original formula of TS method for isotropic materials [26], a mapping from $\overline{\sigma}_{ij}$ to $\widetilde{\sigma}_{ij}$ can be established as below

$$\widetilde{\sigma}_{ij}=\begin{cases}\overline{p}\delta_{ij}+\dfrac{\overline{q}_{\mathrm{c}}}{\overline{q}}\left(\overline{\sigma}_{ij}-\overline{p}\delta_{ij}\right), & (\overline{q}\neq 0)\\ \overline{\sigma}_{ij}, & (\overline{q}=0)\end{cases} \tag{4}$$

where $\overline{p}=\overline{\sigma}_{ii}/3$, $\overline{q}=\sqrt{3\left(\overline{\sigma}_{ij}-\overline{p}\delta_{ij}\right)\left(\overline{\sigma}_{ij}-\overline{p}\delta_{ij}\right)/2}$ are mean stress and deviatoric stress of $\overline{\sigma}_{ij}$, respectively; $\overline{q}_{\mathrm{c}}$ is the deviatoric stress at the triaxial compression state of the yield curve in the deviatoric plane of the modified stress space. The expression of $\overline{q}_{\mathrm{c}}$ should be derived from the failure criterion. For the Lade's criterion which will be used in this paper, $\overline{q}_{\mathrm{c}}$ is expressed as

$$\overline{q}_{\mathrm{c}}=\bar{I}_1\left\{1+\frac{\bar{J}}{2}\left[\cos\left(\frac{1}{3}\cos^{-1}\bar{J}\right)\right]^{-1}\right\} \tag{5}$$

where

$$\bar{J}=-\sqrt{\frac{27\bar{I}_3}{\bar{I}_1^3}} \tag{6}$$

where $\bar{I}_1$ and $\bar{I}_3$ are the first and third invariants of $\overline{\sigma}_{ij}$, respectively. Derivation of $\overline{q}_{\mathrm{c}}$ refers to Ref. [25]. $\overline{q}_{\mathrm{c}}$ can also be derived from other failure criteria such as the SMP criterion [24] and the generalized non-linear strength criterion [37]. But the Lade's criterion fits better with the experimental data in the model verification. Note that $\widetilde{\sigma}_{ij}=\overline{\sigma}_{ij}$ at the triaxial compression state in the modified stress space.

It can be verified from Eq. (4) that after the stress transformation, the following three equations are always satisfied

$$\begin{cases}\widetilde{p}=\overline{p}\\ \widetilde{\theta}=\overline{\theta}\\ \widetilde{q}=\overline{q}_{\mathrm{c}}\end{cases} \tag{7}$$

where $\widetilde{p}=\widetilde{\sigma}_{ii}/3$ and $\widetilde{q}=\sqrt{3\left(\widetilde{\sigma}_{ij}-\widetilde{p}\delta_{ij}\right)\left(\widetilde{\sigma}_{ij}-\widetilde{p}\delta_{ij}\right)/2}$ are mean stress and deviatoric stress of $\widetilde{\sigma}_{ij}$, respectively; $\overline{\theta}$ and $\widetilde{\theta}$ are Lode's angles of $\overline{\sigma}_{ij}$ and $\widetilde{\sigma}_{ij}$, respectively. Eq. (7) demonstrates that the yield/failure curve in the deviatoric plane of the transformed stress space is a circle with its radius being $\overline{q}_{\mathrm{c}}$.

From σ_{ij} to $\overline{\sigma}_{ij}$, the effect of anisotropy is considered; and from $\overline{\sigma}_{ij}$ to $\widetilde{\sigma}_{ij}$, the effect of intermediate principal stress is considered. These two steps of stress transformation can work together, called the anisotropic transformed stress (ATS) method. With the help of $\widetilde{\sigma}_{ij}$, it is much easier to develop failure criteria and constitutive models which can account for the effects of anisotropy and intermediate principal stress together.

5. Anisotropic Lade's criterion

5.1 Criterion expressed in the modified stress space

In the modified stress space, the Lade's criterion can be used to describe the strength of anisotropic soils. Hence, anisotropic Lade's criterion is developed as below

$$\frac{\bar{I}_1^3}{\bar{I}_3} = C \tag{8}$$

where C is a constant independent of loading directions and stress paths. The value of C can be determined by VC test or HC test or any other loading conditions. For VC loading, one can get

$$C = \frac{4\left[3+(3\Delta-1)M_{\mathrm{v}}\right]^3}{\Delta(1-\Delta)^2(3+2M_{\mathrm{v}})(3-M_{\mathrm{v}})^2} \tag{9a}$$

and for HC loading one has

$$C = \frac{\left[6-(3\Delta-1)M_{\mathrm{h}}\right]^3}{2\Delta(1-\Delta)^2(3+2M_{\mathrm{h}})(3-M_{\mathrm{h}})^2} \tag{9b}$$

where M_{v} and M_{h} denote the failure stress ratio q/p ($p=\sigma_{ii}/3$ is mean stress and $q=\sqrt{3(\sigma_{ij}-p\delta_{ij})(\sigma_{ij}-p\delta_{ij})/2}$ is deviatoric stress) in VC test and HC test, respectively. The determination of Δ is discussed in Section 7.1.

In this paper, anisotropy is considered through stress modification. $\bar{\sigma}_{ij}$ contains the information of the material anisotropy and loading direction so that other failure criteria, such as the SMP criterion and the generalized non-linear strength criterion, can also be extended in the same way. Therefore, if $f(\sigma_{ij})=k$ represents the isotropic criteria in which k denotes the material constant, anisotropic criteria can be expressed as $f(\bar{\sigma}_{ij})=k$. In $f(\bar{\sigma}_{ij})=k$, k is still constant and independent of the loading direction. The form of the expression remain unchanged in the modified stress space and only one parameter Δ is added.

5.2 Criterion expressed in the transformed stress space

The anisotropic Lade's criterion can also be expressed using $\tilde{\sigma}_{ij}$ as below

$$\frac{\tilde{q}}{\tilde{p}} = \bar{M} \tag{10}$$

where $\bar{M}$ is the failure stress ratio $\bar{q}/\bar{p}$ in the triaxial compression state of the modified stress space. For cross-anisotropic soils, $\bar{M}$ is a function of M_{v} as follows

$$\bar{M} = \frac{3}{2}\cdot\frac{(3\Delta+1)M_{\mathrm{v}}+(9\Delta-3)}{(3\Delta-1)M_{\mathrm{v}}+3} \tag{11}$$

Note that Eqs. (8) and (10) are essentially equivalent.

Failure criterion can be first established as a simple form (Eq. (10)) in the transformed stress space. Then using the mappings of stress in Eqs. (4) and (2), the failure criterion in the modified stress space and that in the ordinary stress space can be obtained successively. Fig. 3 shows the 3D failure

surfaces of anisotropic Lade's criterion in three stress spaces. The failure surface in the transformed stress space is a cone. In the modified stress space, its cross-section in the deviatoric plane is a curved triangle which is symmetric about all the three principal stress axes, similar to the isotropic Lade's criterion. In the ordinary stress space, it can be seen that the hydrostatic axis locates no longer in the center of the failure surface. The intercepts of its cross-section on three principal stress axes are not the same. So that anisotropy is revealed.

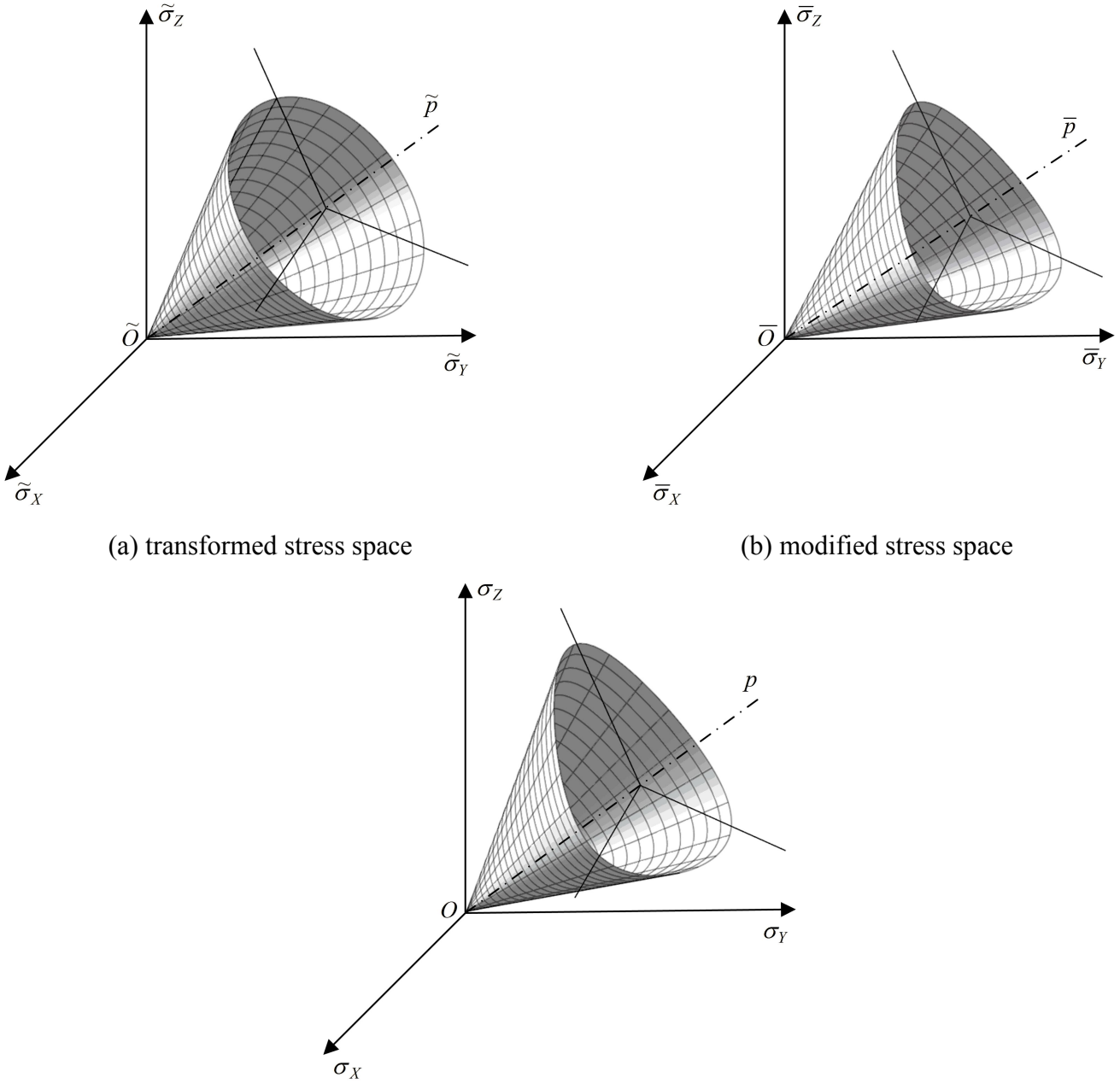

(a) transformed stress space

(b) modified stress space

(c) ordinary stress space

Fig. 3 Failure surfaces in three stress spaces

5.3 Parametric study

The shape of the failure curve in the deviatoric plane of the ordinary stress space is dependent on the degree of fabric anisotropy and loading direction. Two quantities, Δ and δ, can reflect the effects of these two factors, respectively.

Fig. 4 shows a series of failure curves under the loading Case 1. To study the effect of Δ, M_v is supposed to be a constant. The deviatoric plane is divided into three sectors. In Sector Ⅰ, Ⅱ and Ⅲ, σ_Z is the major, intermediate and minor principal stress, respectively. The loading condition at $\theta = 0°$ corresponds to the VC test, those at $\theta = 120°$ and $240°$ correspond to the HC test, and that at $\theta = 180°$ corresponds to the VE test ($\sigma_Z < \sigma_X = \sigma_Y$, triaxial extension with the minor principal stress being parallel to the direction of deposition). The failure curves always pass through the same point on the σ_Z-axis as M_v is constant. The σ_Z-axis is the only axis of symmetry of these curves as the soil is cross-anisotropic. When $\Delta = 1/3$, the soil fabric is isotropic and the failure curve is also isotropic. In this case, the anisotropic Lade's criterion is recovered to the isotropic Lade's criterion (see the broken line in Fig. 4). When $\Delta < 1/3$, the failure curve shrinks at the same θ as the value of Δ decreases. This indicates Δ is a parameter measuring not only the fabric anisotropy but also the strength anisotropy of soils.

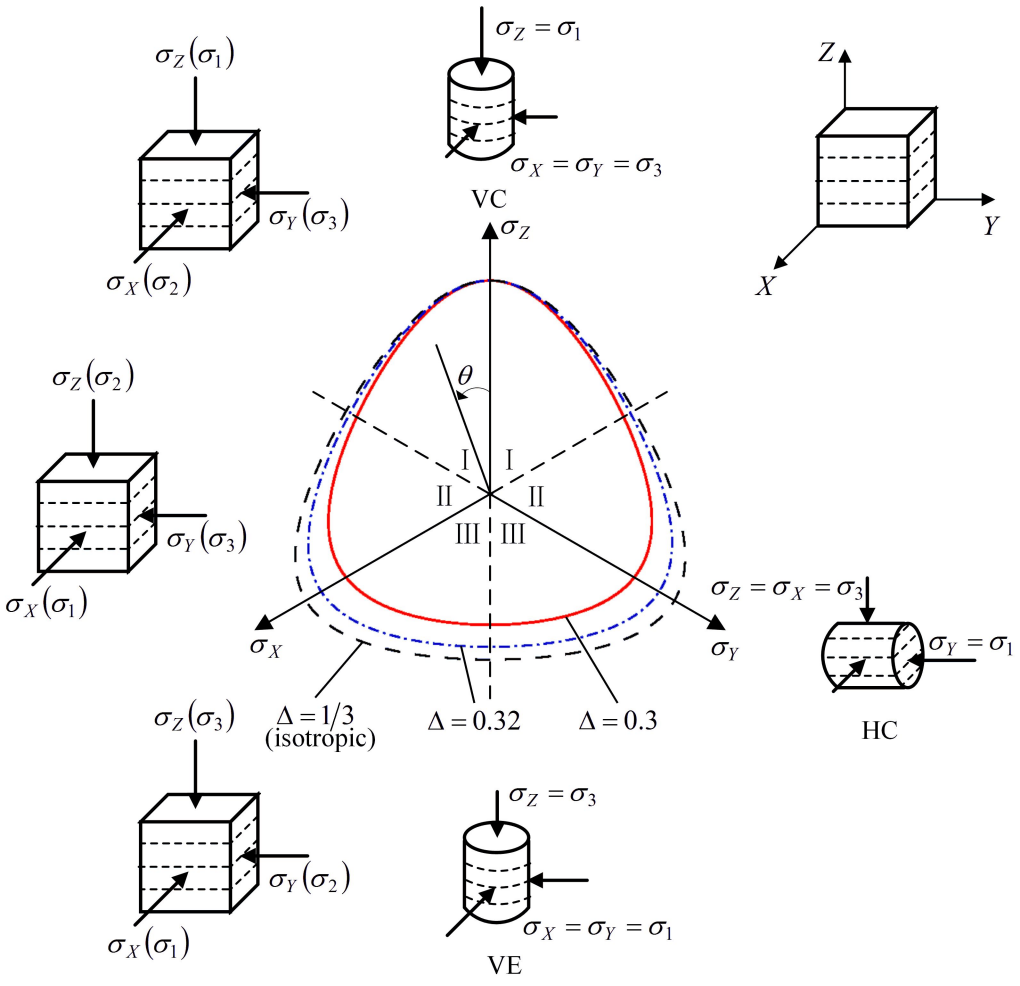

Fig. 4 Effect of the degree of fabric anisotropy on soil strength

Fig. 5 shows the failure curves of anisotropic Lade's criterion with $\Delta = 0.30$ in the loading Case 2. The effect of the loading direction can be observed from these curves. The failure curve is symmetric about the σ_Z -axis when $\delta = 0°$. When the direction of deposition is rotated in the *Y*-*Z* plane, the failure curve becomes symmetric about the σ_X -axis when $\delta = 45°$, and symmetric about the σ_Y -axis when $\delta = 90°$. There are two intersection points for the three curves which lie on the positive and negative sides of the σ_X -axis, respectively.

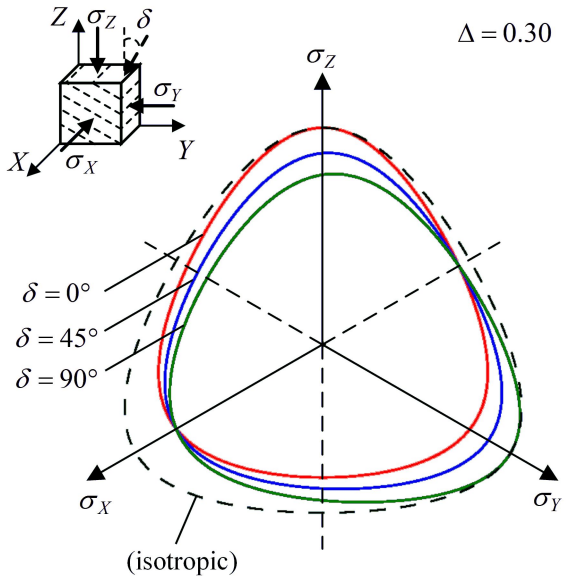

Fig. 5 Effect of the loading direction on soil strength

Fig. 6 shows the relation between the friction angle φ and δ under the triaxial compression state according to the anisotropic Lade's criterion. It can be seen that φ decreases with δ monotonically when the soil is anisotropic. And as the value of Δ decreases, the difference between friction angles of VC and HC tests will enlarge.

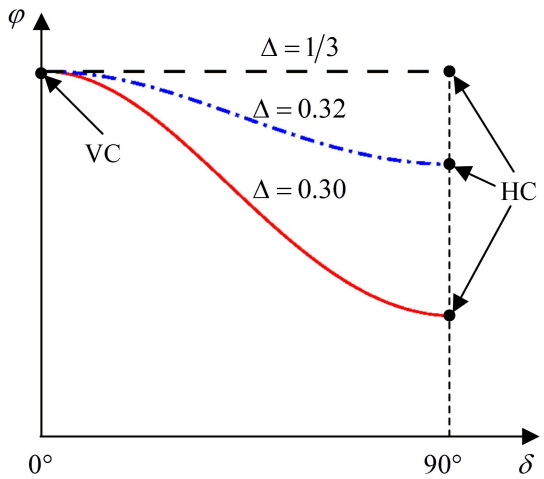

Fig. 6 Variation of φ with δ in the triaxial compression tests

6. Anisotropic UH model

6.1 Isotropic UH model in triaxial compression

As a representative example, the UH (unified hardening) model will be generalized to account for soil anisotropy using the ATS method in this paper. It is helpful to have a brief introduction of the isotropic UH model first. More detailed description of the model can be found in Yao *et al*. [42-43].

The UH model uses an elliptical current yield surface of the same shape as that of the modified Cam-clay model (Fig. 7). The current stress point always lies on the current yield surface. A reference yield surface which is similar to the current yield surface is employed to model the effect of overconsolidation on soil behavior. A radial mapping rule with the mapping center being the origin of the $p-q$ coordinate system is used. In Fig. 7, $\mathrm{B}(p',q')$ is the 'image' stress state for the current stress state $\mathrm{A}(p,q)$. A stress quantity with a prim indicates that it is associated with the reference yield surface in this paper.

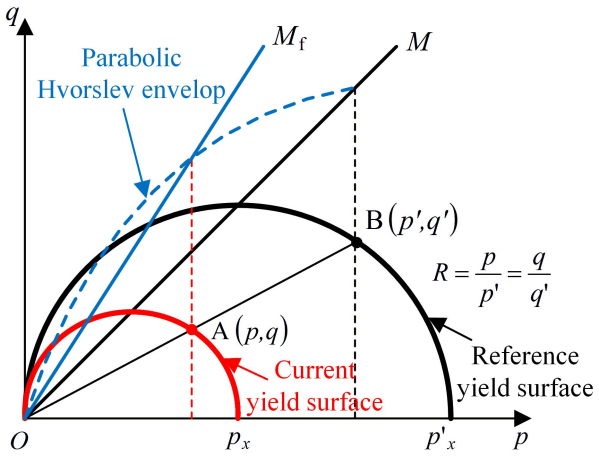

Fig. 7 Yield surfaces of UH model

The following is the expression for the yield surface f and plastic potential g

$$f=g=\ln\frac{p}{p_{x0}}+\ln\left(1+\frac{\eta^2}{M^2}\right)-\frac{1}{c_\mathrm{p}}H=0 \tag{12}$$

where $\eta=q/p$; p_{x0} is the intercept of the current yield surface on the p-axis in the initial condition; M is the critical state ratio of triaxial compression; $c_\mathrm{p}=(\lambda-\kappa)/1+e_0$ where λ and κ are the slope of the normal compression line (NCL) and swelling line in the $e-\ln p$ coordinate system, respectively; e is the void ratio and e_0 represents its initial value. The unified hardening parameter H which is essential for modelling the dilatancy and strain softening of overconsolidated clays is defined as

$$\mathrm{d}H=\frac{M_\mathrm{f}^4-\eta^4}{M^4-\eta^4}\mathrm{d}\varepsilon_\mathrm{v}^\mathrm{p} \tag{13}$$

where $\mathrm{d}\varepsilon_\mathrm{v}^\mathrm{p}$ is the plastic volumetric strain increment and M_f is the potential failure stress ratio.

Since both the zero-tension line and Hvorslev envelope are boundaries that the stress path should not exceed, Yao *et al*. [43] proposed to use a parabolic Hvorslev envelop to model the strength of overconsolidated clays. M_{f} is the stress ratio of the point on the parabolic Hvorslev envelop with the same mean stress as Point $\mathrm{A}(p,q)$ and can be expressed as:

$$M_{\mathrm{f}} = 6\left[\sqrt{\frac{\chi}{R}\left(1+\frac{\chi}{R}\right)}-\frac{\chi}{R}\right] \tag{14}$$

where

$$\chi = \frac{M^2}{12(3-M)} \tag{15}$$

where R measures the degree of overconsolidation at the current stress level (Fig. 7). When the overconsolidation ratio is infinite ($R \to 0$), $M_{\mathrm{f}} = 3$ which is the slope of the zero-tension line; while at the critical state, soil turns to be normally consolidated ($R = 1$) and M_{f} is equal to M .

The reference yield surface f' is expressed as

$$f' = \ln\frac{p'}{p'_{x0}} + \ln\left(1+\frac{\eta^2}{M^2}\right) - \frac{1}{c_{\mathrm{p}}}\varepsilon_{\mathrm{v}}^{\mathrm{p}} = 0 \tag{16}$$

where p'_{x0} is the intercept of the reference yield surface on the p -axis in the initial condition. f' represents the normally consolidated state of the soil and adopts plastic volumetric strain $\varepsilon_{\mathrm{v}}^{\mathrm{p}}$ as its hardening parameter. The attenuation of overconsolidation during loading is reflected by the evolution of these two surfaces. Based on the expressions for the current yield surface, reference yield surface and mapping rule, one can get the overconsolidation parameter R as below

$$R = \frac{p}{p'} = \frac{p}{p'_{x0}}\left(1+\frac{\eta^2}{M^2}\right)\exp\left(-\frac{\varepsilon_{\mathrm{v}}^{\mathrm{p}}}{c_{\mathrm{p}}}\right) \tag{17}$$

The initial value of R equals to the reciprocal of the overconsolidation ratio (OCR) when the soil has been subjected to isotropic compression. R increases with the loading and reaches the maximum value of 1 at the critical state.

6.2 Anisotropic UH model

Without changing the model framework, the UH model can be readily extended to account for the influence of anisotropy and intermediate principal stress at one time when σ_{ij} in the formulations is replaced by $\widetilde{\sigma}_{ij}$. In the transformed stress space, the expressions for the current yield surface, plastic potential and reference yield surface of the anisotropic UH model are

$$f = g = \ln\frac{\widetilde{p}}{\widetilde{p}_{x0}} + \ln\left(1+\frac{\widetilde{\eta}^2}{\overline{M}^2}\right) - \frac{1}{c_{\mathrm{p}}}\widetilde{H} = 0 \tag{18}$$

$$f' = \ln\frac{\widetilde{p}'}{\widetilde{p}'_{x0}} + \ln\left(1+\frac{\widetilde{\eta}^2}{\overline{M}^2}\right) - \frac{1}{c_\mathrm{p}}\varepsilon_\mathrm{v}^\mathrm{p} = 0 \tag{19}$$

where $\widetilde{\eta} = \widetilde{q}/\widetilde{p}$; $\widetilde{p}_{x0}$ and $\widetilde{p}'_{x0}$ are the intercepts of the initial current/reference yield surface on the $\widetilde{p}$-axis, respectively. Evolution law for $\widetilde{H}$ is

$$\mathrm{d}\widetilde{H} = \frac{\widetilde{M}_\mathrm{f}^4 - \widetilde{\eta}^4}{\overline{M}^4 - \widetilde{\eta}^4}\mathrm{d}\varepsilon_\mathrm{v}^\mathrm{p} \tag{20}$$

The slope of the zero-tension line in the modified/transformed stress space is still 3. As a result, substituting $\overline{M}$ for M, the potential failure stress ratio $\widetilde{M}_\mathrm{f}$ is obtained as below

$$\widetilde{M}_\mathrm{f} = 6\left[\sqrt{\frac{\overline{\chi}}{\widetilde{R}}\left(1+\frac{\overline{\chi}}{\widetilde{R}}\right)} - \frac{\overline{\chi}}{\widetilde{R}}\right] \tag{21}$$

where

$$\overline{\chi} = \frac{\overline{M}^2}{12\left(3-\overline{M}\right)} \tag{22}$$

The overconsolidation parameter $\widetilde{R}$ is still derived from the reference yield function in Eq. (19) as below

$$\widetilde{R} = \frac{\widetilde{p}}{\widetilde{p}'_{x0}}\left(1+\frac{\widetilde{\eta}^2}{\overline{M}^2}\right)\exp\left(-\frac{\varepsilon_\mathrm{v}^\mathrm{p}}{c_\mathrm{p}}\right) \tag{23}$$

The original UH model and anisotropic UH model are compared in Table 1. It can be seen that the form of the formulations including yield function, plastic potential and hardening parameter in the anisotropic UH model remain the same with those of the original UH model.

From the derivation of the elastoplastic constitutive tensor D_{ijkl} (shown in the Appendix), it can be seen that no more extra items is added to D_{ijkl} compared with the general form of D_{ijkl}. It is worth mentioning that $\widetilde{\sigma}_{ij}$ just provides a mathematical tool for the convenience of developing 3D constitutive models. Each part of D_{ijkl} can be expressed in terms of σ_{ij} explicitly, as $\widetilde{\sigma}_{ij}$ is an explicit function of σ_{ij}. Therefore, the constitutive equation $\mathrm{d}\sigma_{ij} = D_{ijkl}\mathrm{d}\varepsilon_{kl}$ is still a function of σ_{ij}, like all the other constitutive models.

6.3 Yield surfaces and loading-unloading criterion

The current yield surfaces of the anisotropic UH model in three stress spaces are plotted in Fig. 8. On these surfaces, the longitude lines can be regarded as yield curves in the meridian planes with different values of Lode's angle, while the latitude lines can be regarded as yield curves in the deviatoric planes with different values of mean stress. The 3D yield surface in the transformed stress

in Fig. 8a is plotted according to Eq. (18). It can be seen that the yield surface is an ellipsoid which is symmetric about the $\widetilde{p}$ -axis. If $\widetilde{\sigma}_{ij}$ in Eq. (18) is replaced by the function of $\overline{\sigma}_{ij}$ in Eq. (4), the yield function in the modified stress space can be obtained and then the yield surface is plotted in Fig. 8b. The yield curves in the meridian planes shrink as the intermediate principal stress coefficient increases. And the shape of the yield curve in the deviatoric plane is similar to a circle at a low value of the stress ratio $\overline{q}/\overline{p}$, and to a triangle if the ratio is high, which correspond to the Lade's criterion. Using the relation of σ_{ij} and $\overline{\sigma}_{ij}$ in Eq. (2), a 3D yield surface, which can reflect the effect of anisotropy, is plotted in the ordinary stress space as shown in Fig. 8c. The yield surface is not symmetric about the hydrostatic axis due to the existence of anisotropy. The direction and degree of this inclination is related to the loading direction and the degree of anisotropy.

Table 1. Comparison of the original UH model with the anistropic UH model

	Original UH model	Anisotropic UH model
Stress tensor	σ_{ij}	$\widetilde{\sigma}_{ij}=\overline{p}\delta_{ij}+\frac{\overline{q}_{\mathrm{c}}}{\overline{q}}\left(\overline{\sigma}_{ij}-\overline{p}\delta_{ij}\right)$ where $\overline{\sigma}_{ij}=\frac{3}{2}\left(\sigma_{ik}F_{kj}+F_{ik}\sigma_{kj}\right)$
Strain tensor	$\mathrm{d}\varepsilon_{ij}=\mathrm{d}\varepsilon_{ij}^{\mathrm{e}}+\mathrm{d}\varepsilon_{ij}^{\mathrm{p}}$	
Elastic strain	$\mathrm{d}\sigma_{ij}=D_{ijkl}^{\mathrm{e}}\mathrm{d}\varepsilon_{kl}^{\mathrm{e}}$	
Failure criterion	$\frac{q}{p}=M$	$\frac{\widetilde{q}}{\widetilde{p}}=\overline{M}$
Constitutive model	$f=g=\ln\frac{p}{p_{x0}}+\ln\left(1+\frac{\eta^2}{M^2}\right)-\frac{H}{c_{\mathrm{p}}}=0$	$f=g=\ln\frac{\widetilde{p}}{\widetilde{p}_{x0}}+\ln\left(1+\frac{\widetilde{\eta}^2}{\overline{M}^2}\right)-\frac{\widetilde{H}}{c_{\mathrm{p}}}=0$
Hardening parameter	$\mathrm{d}H=\frac{M_{\mathrm{f}}^4-\eta^4}{M^4-\eta^4}\mathrm{d}\varepsilon_{\mathrm{v}}^{\mathrm{p}}$	$\mathrm{d}\widetilde{H}=\frac{\widetilde{M}_{\mathrm{f}}^4-\widetilde{\eta}^4}{\overline{M}^4-\widetilde{\eta}^4}\mathrm{d}\varepsilon_{\mathrm{v}}^{\mathrm{p}}$
Potential failure stress ratio	$M_{\mathrm{f}}=6\left[\sqrt{\frac{\chi}{R}\left(1+\frac{\chi}{R}\right)}-\frac{\chi}{R}\right]$	$\widetilde{M}_{\mathrm{f}}=6\left[\sqrt{\frac{\overline{\chi}}{\widetilde{R}}\left(1+\frac{\overline{\chi}}{\widetilde{R}}\right)}-\frac{\overline{\chi}}{\widetilde{R}}\right]$
Overconsolidation parameter	$R=\frac{p}{p'_{x0}}\left(1+\frac{\eta^2}{M^2}\right)\exp\left(-\frac{\varepsilon_{\mathrm{v}}^{\mathrm{p}}}{c_{\mathrm{p}}}\right)$	$\widetilde{R}=\frac{\widetilde{p}}{\widetilde{p}'_{x0}}\left(1+\frac{\widetilde{\eta}^2}{\overline{M}^2}\right)\exp\left(-\frac{\varepsilon_{\mathrm{v}}^{\mathrm{p}}}{c_{\mathrm{p}}}\right)$
Flow rule	$\mathrm{d}\varepsilon_{ij}^{\mathrm{p}}=\Lambda\frac{\partial g}{\partial\sigma_{ij}}$	$\mathrm{d}\varepsilon_{ij}^{\mathrm{p}}=\Lambda\frac{\partial g}{\partial\widetilde{\sigma}_{ij}}$

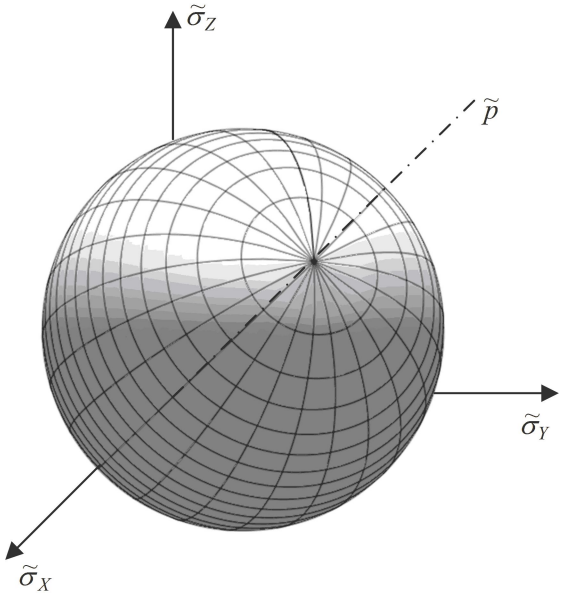

(a) transformed stress space

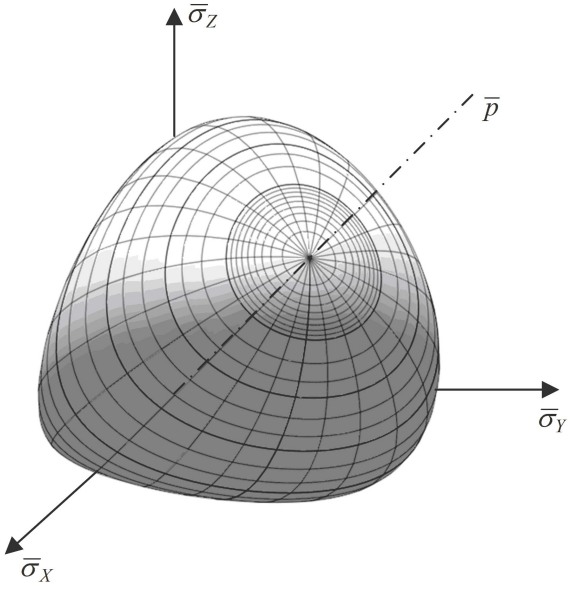

(b) modified stress space

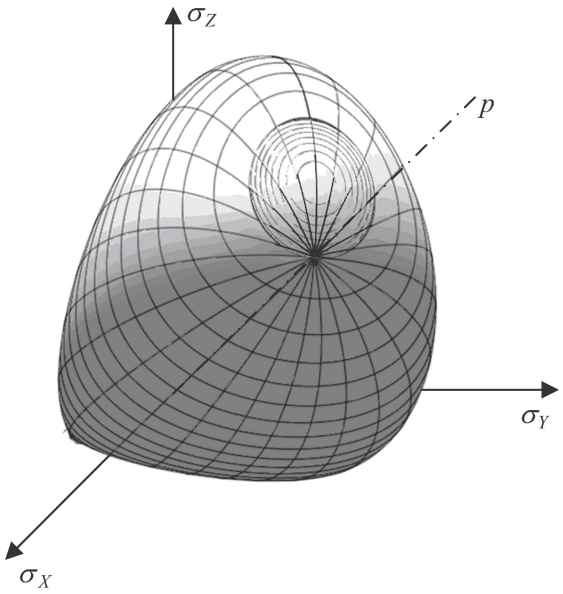

(c) ordinary stress space

Fig. 8 Yield surfaces in three stress spaces

Yield curves and critical state lines (CSLs) in the meridian plane on which the Lode's angle equals to $0°$ (VC loading) and $180°$ (VE loading) in three stress spaces are shown in Fig. 9. In the transformed stress space, the yield curve is an ellipse symmetric about the horizontal axis (Fig. 9a) and the slope of CSLs of VC and VE loading are equal. In the modified stress space, the yield curve in the extension side shrinks while the yield curve in the compression side is the same as that in the transformed stress space since $\widetilde{\sigma}_{ij} = \overline{\sigma}_{ij}$ at the triaxial compression state (Fig. 9b). It can be seen in Fig. 9c that in the ordinary stress space, the yield curve rotates upwards from the p -axis. The rotation angle of the yield curve will be larger as the degree of anisotropy increases (smaller value of Δ). This kind of yield curve conforms to the general cognition of the yielding of anisotropic soils

[44-45].

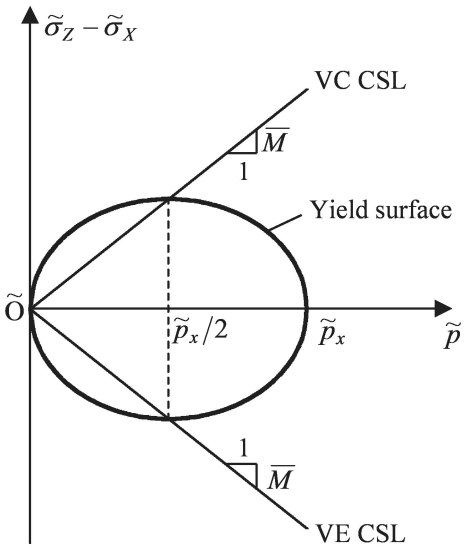

(a) transformed stress space

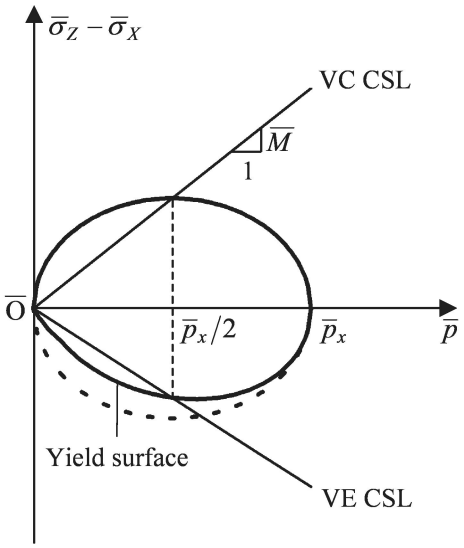

(b) modified stress space

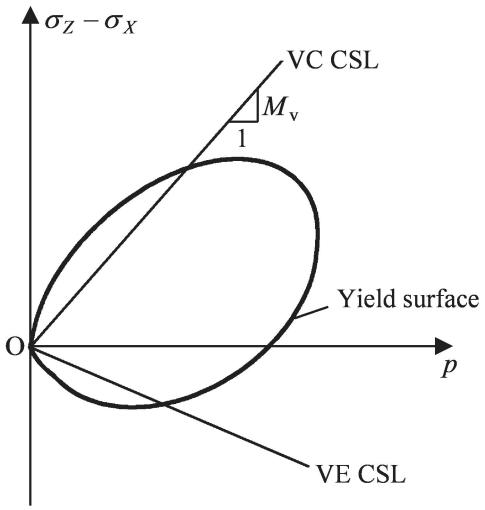

(c) ordinary stress space

Fig. 9 Yield curves in the meridian plane of three stress spaces

The judgment of loading or unloading is conducted in the transformed stress space as below

$$\begin{cases} \mathrm{d}\widetilde{p}_x > 0 & \text{loading (hardening)} \\ \mathrm{d}\widetilde{p}_x \le 0 \begin{cases} \widetilde{M}_\mathrm{f} \le \widetilde{\eta} & \text{loading (softening)} \\ \widetilde{M}_\mathrm{f} > \widetilde{\eta} & \text{unloading} \end{cases} \end{cases} \tag{24}$$

where $\widetilde{p}_x$ is the intercept of the current yield surface in the transformed stress space on the $\widetilde{p}$-axis.

It is necessary to explain why the anisotropic soil shows higher stiffness and lower axial strain to failure in VC test than those in HC test based on the anisotropic UH model. Suppose VC test is

conducted from the isotropic consolidation state ($\sigma_Z = \sigma_X = \sigma_Y$), one has $\overline{\sigma}_Z < \overline{\sigma}_X = \overline{\sigma}_Y$ at the very beginning according to Eq. (3a) since $\Delta < 1/3$. As the loading continues, $\overline{\sigma}_Z$ increases and gets closer to $\overline{\sigma}_X$ and $\overline{\sigma}_Y$. The deviatoric stress of the modified or transformed stress tensor decreases first so that the current yield surface will shrink. According to the loading-unloading criterion, the sample will experience elastic unloading and turn to be overconsolidated. Therefore, the initial stiffness is high and the strain to failure is low in VC test. And after reaching the peck strength, strain-softening might occur even though the soil is originally normally consolidated, if the degree of anisotropy is large enough. This theory can be used to explain the strain-softening of anisotropically normally consolidated Kawasaki clay in triaxial compression tests [1].

7. Model verification

7.1 Parameter determination

There are five parameters in the anisotropic UH model: $\overline{M}$, λ , κ , ν and Δ . Among them, the first four parameters are inherited from the original UH model. The following is the method of parameter determination.

(1) Δ : Δ measures the degree of fabric anisotropy and should have been determined according to the microscopic statistics of every particle or particle cluster in the sample. But for lack of relevant data, it is recommended that Δ should be determined based on the strength anisotropy. According to the strengths of VC and HC loading, Δ can be obtained as below by combining Eqs. (9a) and (9b)

$$\Delta = \frac{1}{3} - \frac{2(1-a)}{2M_{\mathrm{v}} + aM_{\mathrm{h}}} \tag{25}$$

where

$$a = \left[\frac{(3+2M_{\mathrm{v}})(3-M_{\mathrm{v}})^2}{(3+2M_{\mathrm{h}})(3-M_{\mathrm{h}})^2} \right]^{\frac{1}{3}} \tag{26}$$

(2) $\overline{M}$: After Δ is determined, $\overline{M}$ can be readily obtained based on Eq. (11).

(3) λ : Theoretically, λ should be determined according to the results of test in which the modified stress states satisfy the isotropic compression condition ($\overline{\sigma}_Z = \overline{\sigma}_X = \overline{\sigma}_Y$). λ is the slope of NCL in the $e - \ln \overline{p}$ diagram. But this stress path is difficult to achieve via conventional tests. Investigations show that $e - \ln p$ curves obtained by compression tests in which stress ratios σ_Z / σ_X are kept to be different constants are a series of parallel lines for normally consolidated clays, which means that the values of λ are the same. In fact, isotropic compression test in the ordinary stress space ($\sigma_Z = \sigma_X = \sigma_Y$) is equivalent to a test in which the ratio of modified stresses $\overline{\sigma}_Z / \overline{\sigma}_X$ is equal to a certain value. Therefore, λ can be still determined conveniently by the isotropic compression test.

(4) κ and ν : κ is the slope of the swelling line in the $e - \ln \overline{p}$ diagram, and ν is the Poisson's ratio. Both of them describe the elastic properties of soils. Data from the isotropic

compression test showed that the elastic components of strains of anisotropic soils could be considered to be isotropic [46]. Thus, κ can be determined by the isotropic compression test together with λ.

7.2 Model prediction of strength anisotropy of soils

A series of drained true triaxial tests were carried out on normally consolidated San Francisco Bay Mud [6]. The experimental results are projected in the same deviatoric plane with $I_1 = 500\text{kPa}$ (Fig. 10a). Fig. 10 shows the comparison between the test data and the predictions of both the isotropic Lade's criterion and anisotropic Lade's criterion. The parameters are listed in Fig. 10a. φ_v and φ_h are friction angles measured by VC test and HC test, respectively, with $M_v = 6\sin\varphi_v/(3-\sin\varphi_v)$ and $M_h = 6\sin\varphi_h/(3-\sin\varphi_h)$. According to Eqs. (25), (26) and (11), one can get $\Delta = 0.311$ and $\overline{M} = 1.11$. Note that only φ_v is used to determine the parameter for the isotropic criterion. From Fig. 10a, it can be seen that the anisotropic Lade's criterion provides a good fit for strengths in all the three sectors, with the failure points being distributed evenly on the two sides of the predicted failure curve. Fig. 10b shows the relationship between the friction angle φ and the intermediate principal stress coefficient b $[=(\sigma_2-\sigma_3)/(\sigma_1-\sigma_3)]$. The anisotropic Lade's criterion is able to reflect the influence of anisotropy on φ and the differences between the predicted and measured values are less than $2°\sim 3°$. The isotropic failure criterion only captures the test data in the Sector Ⅰ where the effect of soil anisotropy on failure is negligible.

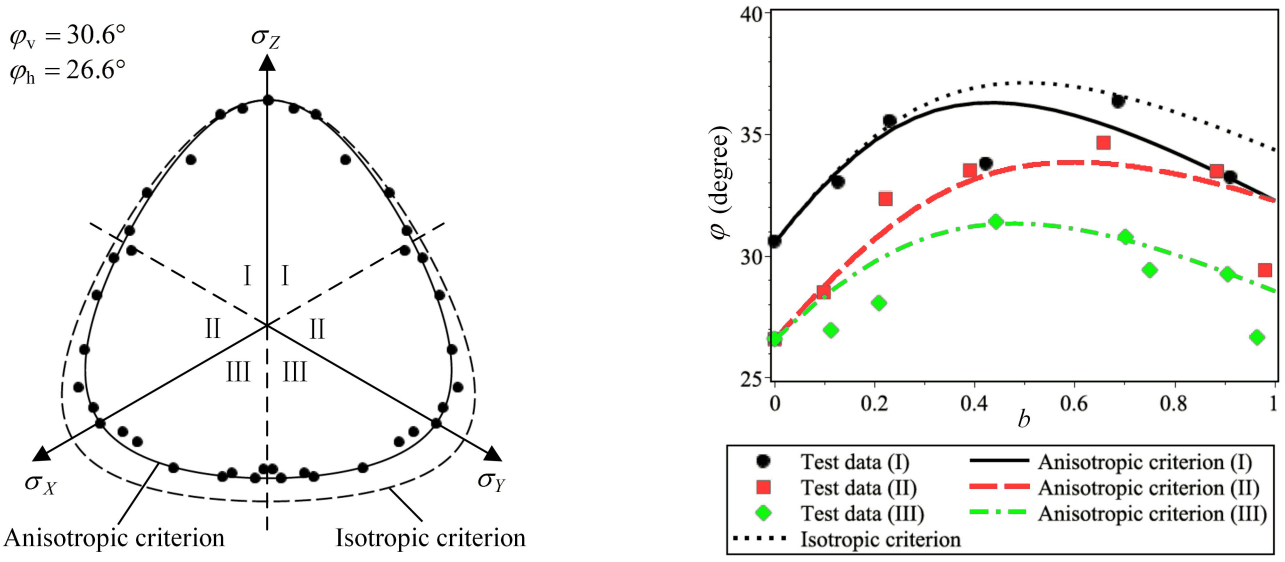

(a) Failure curves in the deviatoric plane (b) φ-b

Fig. 10 Comparisons of the anisotropic and isotropic Lade's criterion with the data from true triaxial tests for San Francisco Bay Mud (data from Kirkgard and Lade, 1993)

Predictions of the isotropic and anisotropic Lade's criteria are also compared with the true triaxial test data for dense Santa Monica Beach sand [47] in Fig. 11. The results are projected in the same

deviatoric plane with $I_1 = 600\text{kPa}$. The parameters are listed in Fig. 11a, and one can get $\Delta = 0.316$ and $\overline{M} = 1.81$ using the same method as that for the San Francisco Bay Mud. As shown in Fig. 11a, there is good agreement between the anisotropic criterion prediction and test data in Sector Ⅰ and Sector Ⅱ of the deviatoric plane. Both the anisotropic and isotropic criteria overestimate the soil strength in Sector Ⅲ while the anisotropic criterion gives better prediction. Fig. 11b indicates that the anisotropic criterion reflects the relative magnitudes of friction angles in three sectors basically and gives good prediction when b is close to 0 or 1. Nevertheless, in the midrange of b -values, friction angles are overestimated. Lade [17] attributed it to the effect of shear banding in the hardening regime which may have reduced the strength of sand. Were the deformation uniform in this b range, the friction angles could have reached the predictions of the anisotropic criterion.

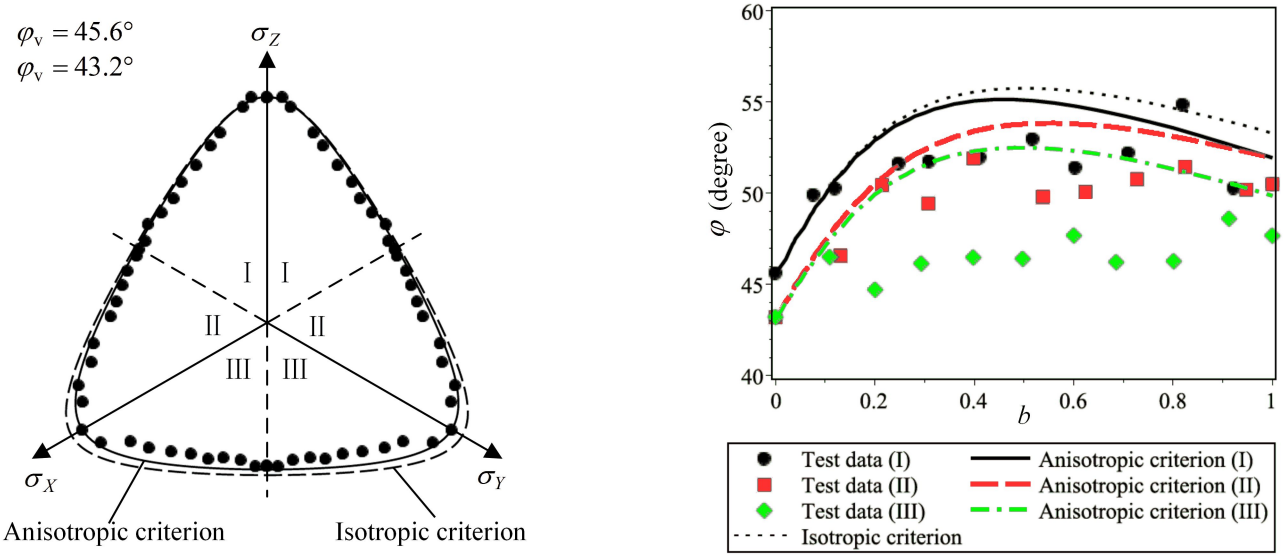

(a) Failure curves in the deviatoric plane (b) φ-b

Fig. 11 Comparisons of the anisotropic and isotropic Lade's criterion with the data from true triaxial tests for Santa Monica Beach sand (data from Abelev and Lade, 2004)

7.3 Model prediction of deformation anisotropy of soils

7.3.1 Isotropic compression test on Nevada sand

Isotropic compression tests were performed on Nevada sand to study its cross-anisotropic behavior [7]. The samples were prepared by funnel deposition followed by tapping in order to produce large degree of anisotropy. The relative density was controlled to be around 30%. During the test, the sample was first isotropically compressed until p reaches over 1800kPa and then unloaded. Isotropic and anisotropic UH models are used to predict the stress-strain relation. It should be mentioned that an elliptical yield surface intersecting the p-axis is not suitable for modelling sand response under general loading conditions, especially when the stress path follows the yield curve closely, because sand is very sensitive to stress ratio changes. In this test, $\eta = 0$ and $\tilde{\eta}$ are both kept low and constant and it is found that the UH model is able to predict the anisotropic deformation

of the sand sample approximately. Fig. 12a and Fig. 12b show the variations of the volumetric strain ε_v and the principal strain along the direction of deposition ε_a with p, respectively. The solid line is the prediction of the anisotropic UH model while the dotted line is that of the isotropic UH model. Parameters used in the anisotropic UH model are listed in Table 2, and the same parameters are used in the isotropic model except $\Delta = 1/3$. In the $\varepsilon_v - p$ diagram, predictions of these two models are almost coincident because $p = \bar{p} = \tilde{p}$ in the isotropic compression stress state. But according to the isotropic model, the predicted ε_a always equals to one third of ε_v, which is far from the experimental data. Using a certain value of Δ, good prediction of ε_a can be got according to the anisotropic UH model while maintaining reasonable prediction of ε_v.

Table 2. Summary of model parameters in this paper

Materials	$\overline{M}$	λ	κ	ν	Δ	e_0
Loose Nevada sand (Lade et al., 2005)	1.68	0.022	0.007	0.30	0.280	0.772
Lightly overconsolidated Kaolin clay (Mitchell, 1972)	0.87	0.14	0.05	0.20	0.326	0.8
K_0 normally consolidated and overconsolidated Kaolin clay (Stipho, 1978)	1.08 1.03	0.14	0.05	0.20	0.325 0.310	0.950~ 1.094

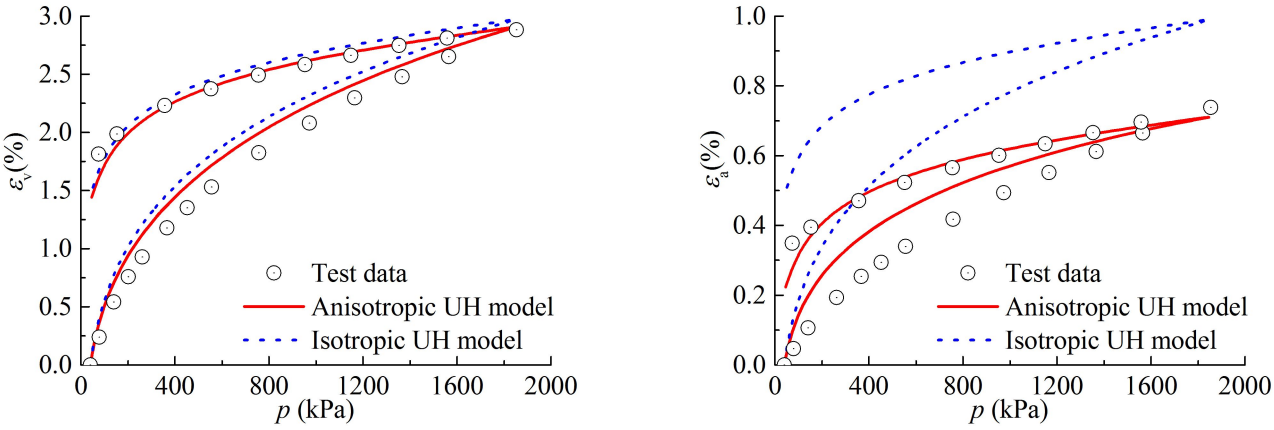

(a) volumetric strain (b) axial strain

Fig. 12 Comparisons of the anisotropic and isotropic UH models with the data from isotropic compression tests of Nevada sand (data from Lade and Abelev, 2005)

7.3.2 Triaxial tests on isotropically consolidated Kaolin clay

Fig. 13 shows the comparison between the anisotropic UH model prediction and experimental data on Kaolin clay [48]. The samples were lightly overconsolidated and trimmed along the vertical and horizontal directions. Parameters are listed in Table 2. Among them, λ and κ are determined

according to the values suggested by Banerjee and Yousif [49]. In order to determine $\overline{M}$ and Δ, M_v and M_h are first obtained based on the deviatoric stresses and pore pressures at the critical state. Then Δ is calculated by Eqs. (25) and (26), and $\overline{M}$ is calculated by Eq. (11). The model gives good simulation of the $\varepsilon_a - q$ relations and effective stress paths but slightly overestimates the excess pore pressure u for both samples. Nevertheless, the anisotropic UH model is capable of capturing the trend that the vertical sample shows higher stiffness and undrained shear strength. In addition, it is interesting to note that the development of excess pore pressure is basically independent of the loading direction, which is well captured by the anisotropic UH model.

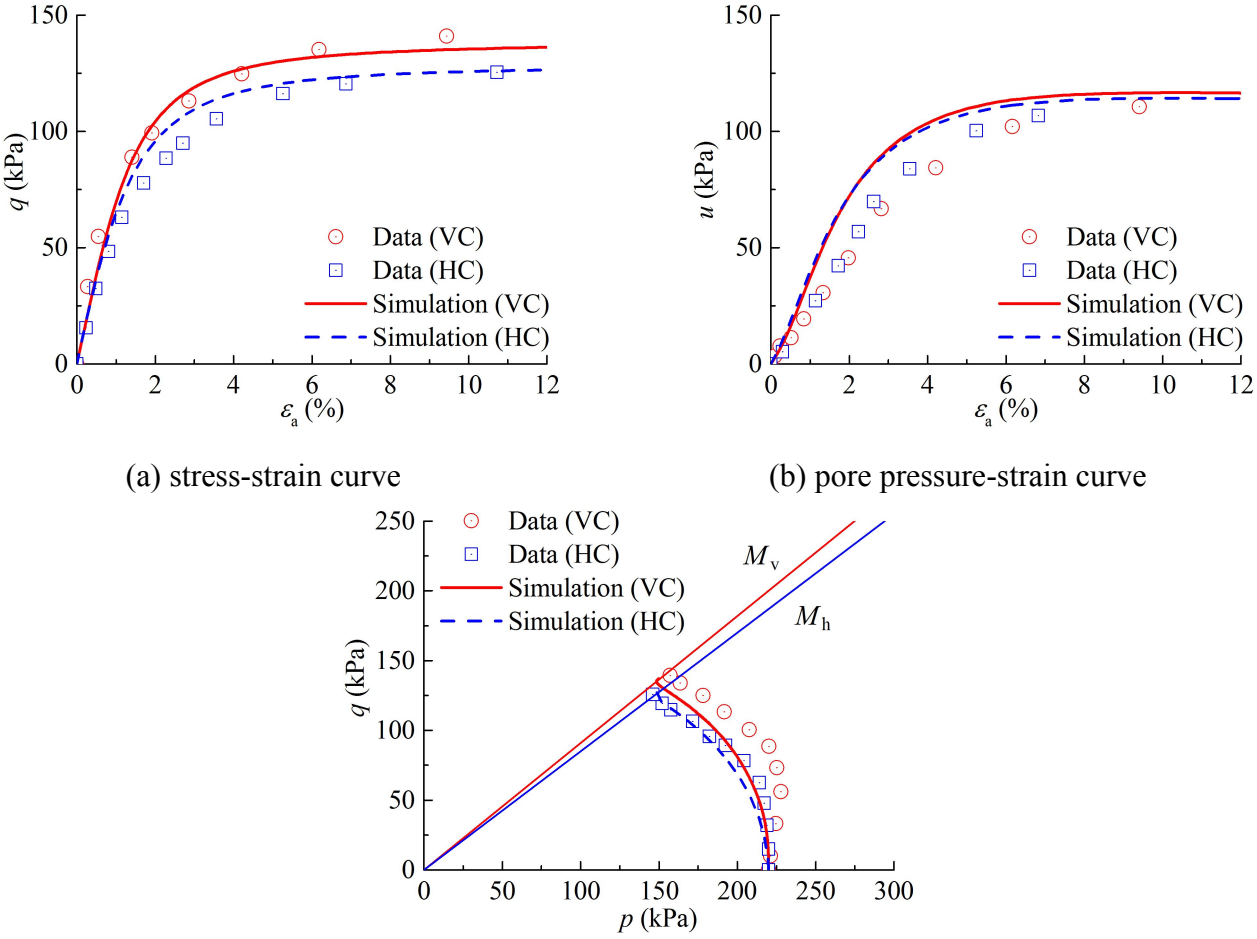

(a) stress-strain curve

(b) pore pressure-strain curve

(c) effective stress path

Fig. 13 Comparisons of the anisotropic UH model with the data from undrained VC and HC tests of isotropically consolidated Kaolin clay (data from Mitchell, 1972)

7.3.3 Triaxial tests on anisotropically consolidated Kaolin clay

A series of undrained triaxial compression and extension tests are conducted on K_0-consolidated Kaolin clay with different initial OCRs by Stipho [50]. The total confining pressure was kept constant in all the tests. Comparison between the predictions of the anisotropic UH model and test data is shown in Fig. 14 ($K_0 = 1.25$) and Fig. 15 ($K_0 = 1.5$). In the Figs. 14 and 15, p_c is the the

mean preconsolidation pressure. Parameters used in the model are shown in Table 2. Among them, the value of Δ is determined based on the strength of VC and VE tests at $OCR = 1$. From these figures, good agreement between the model predictions and test data can be observed.

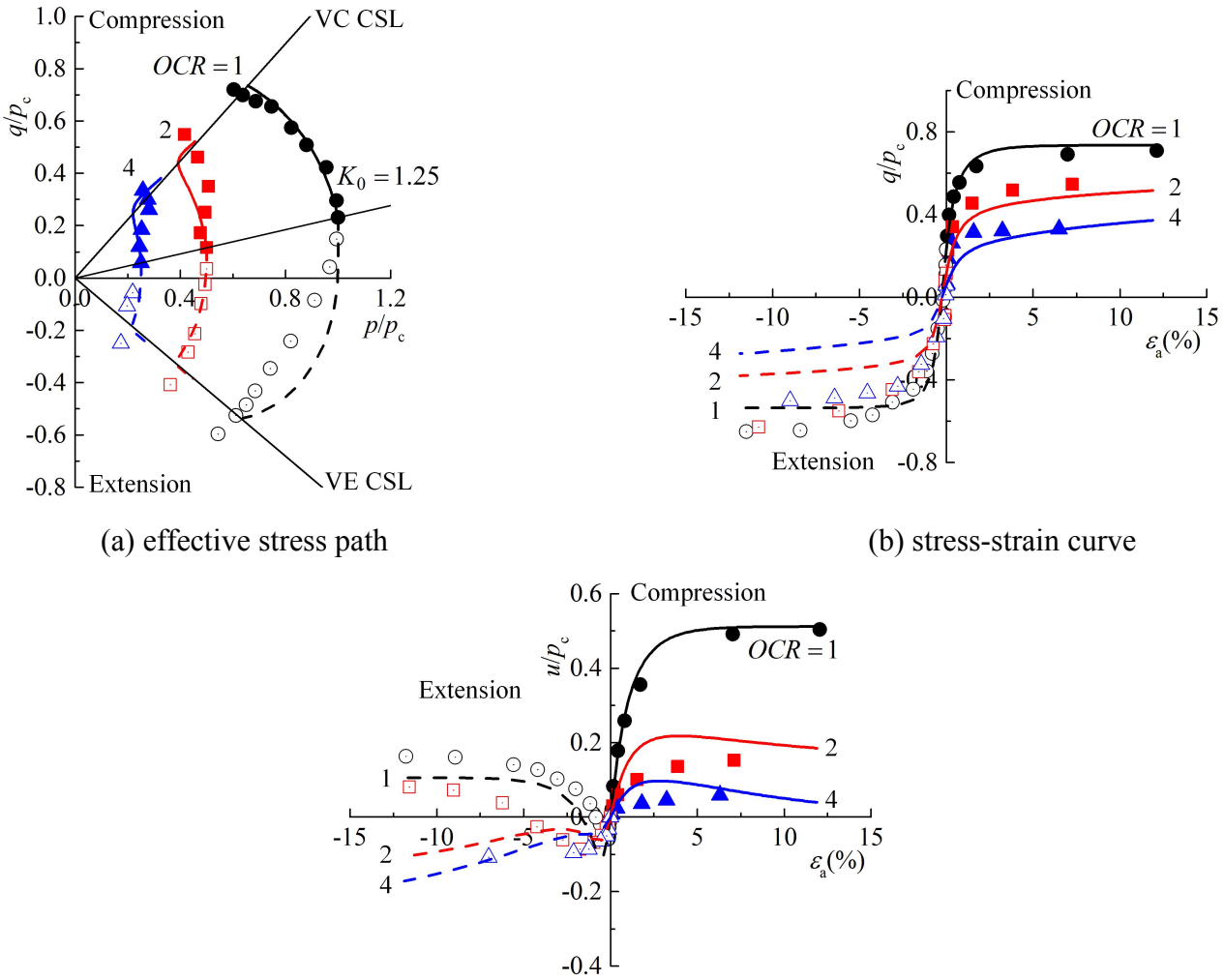

(a) effective stress path

(b) stress-strain curve

(c) pore pressure-strain curve

Fig. 14 Comparisons of the anisotropic UH model with the data from VC and VE tests of K_0-consolidated Kaolin clay with different initial OCRs (K_0=1.25, data from Stipho, 1978)

8. Conclusions and Prospects

The ATS method is proposed in this paper. It includes two steps of stress transformation to account for the effect of anisotropy and intermediate principal stress on the mechanical behaviors of soils. The concrete formulas of the ATS method are summarized in Fig. 1. The Lade's criterion is extended to be anisotropic. The anisotropic Lade's criterion can describe the effect of fabric anisotropy and loading direction on soil strength. The anisotropic UH model is developed by replacing σ_{ij} in the original UH model with $\tilde{\sigma}_{ij}$. The form of the original model formulations including yield function, plastic potential and hardening law remain unchanged. The shear yield and shear failure of soils are described by the anisotropic Lade's criterion. Compared with the original UH model, only one soil

anisotropy parameter Δ, which can be easily obtained using laboratory tests, is added. The other parameters are all independent of the loading direction. Good agreement between the model predictions and test results is observed.

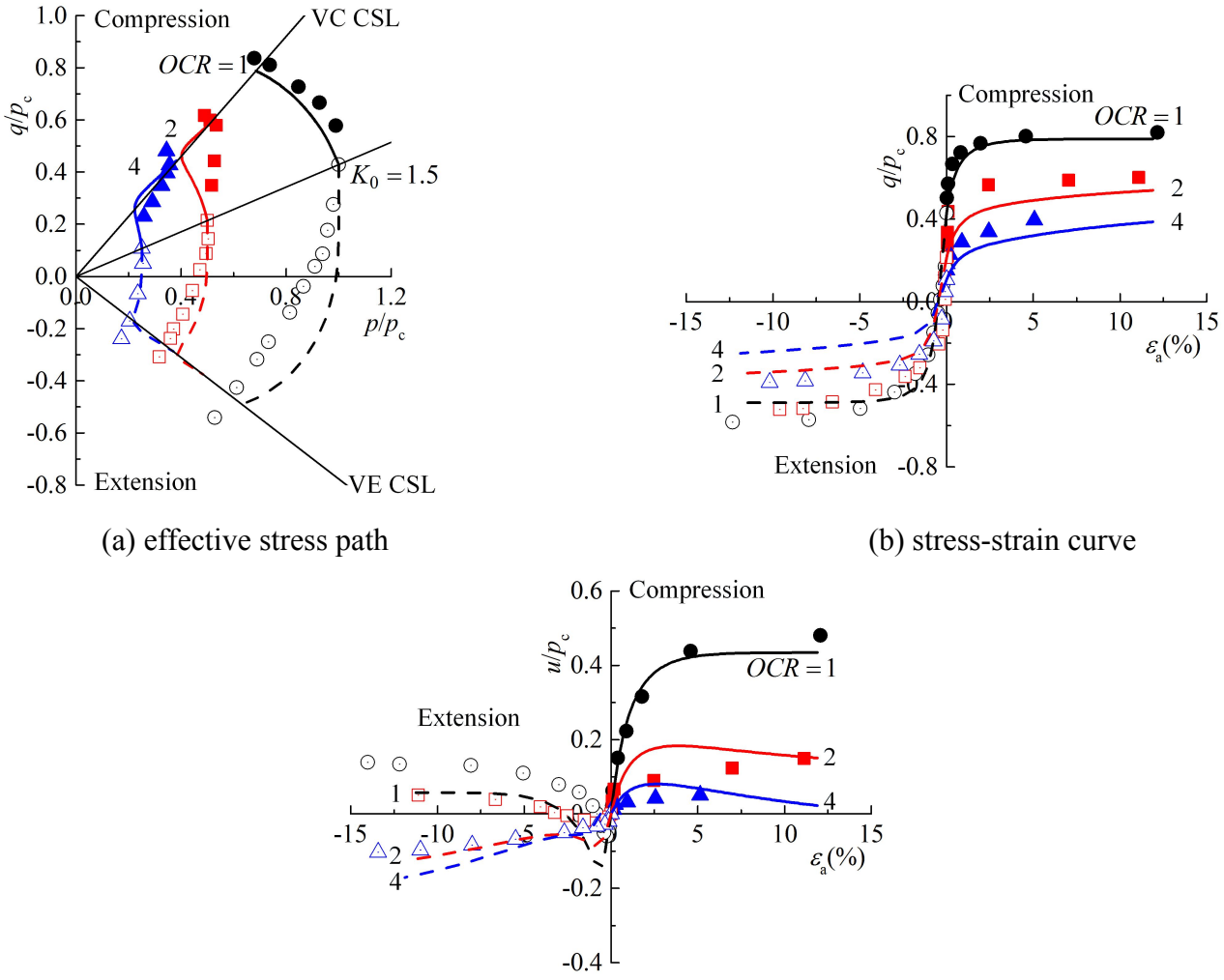

(a) effective stress path

(b) stress-strain curve

(c) pore pressure-strain curve

Fig. 14 Comparisons of the anisotropic UH model with the data from VC and VE tests of K_0-consolidated Kaolin clay with different initial *OCR*s (K_0=1.5, data from Stipho, 1978)

Since the transformed stress tensor used in the model formulations is a function of the modified stress tensor which is a direct multiplication of the stress tensor and fabric tensor, the model response is always dependent on the fabric. However, there are aspects of soil response which do not depend on the material fabric. For example, the critical state stress ratio is found to be almost independent of fabric anisotropy [11]. The proposed method cannot describe this. More work will be done to fully consider different aspects of constitutive response of anisotropic soils in the future.

Appendix: Derivation of elastoplastic constitutive tensor

The elastic components of strains are considered to be isotropic, so that according to the Hooke's law,

the relationship between the stress increment $\mathrm{d}\sigma_{ij}$ and the elastic strain increment $\mathrm{d}\varepsilon_{ij}^{\mathrm{e}}$ is given as

$$\mathrm{d}\sigma_{ij} = D_{ijkl}^{\mathrm{e}}\mathrm{d}\varepsilon_{kl}^{\mathrm{e}} = D_{ijkl}^{\mathrm{e}}\left(\mathrm{d}\varepsilon_{kl} - \mathrm{d}\varepsilon_{kl}^{\mathrm{p}}\right) \tag{A1}$$

where $\mathrm{d}\varepsilon_{ij}$ = total strain increment; $\mathrm{d}\varepsilon_{ij}^{\mathrm{p}}$ = plastic strain increment; and D_{ijkl}^{e} = elastic constitutive tensor, which is expressed by

$$D_{ijkl}^{\mathrm{e}} = \left(K - \frac{2}{3}G\right)\delta_{ij}\delta_{kl} + G\left(\delta_{ik}\delta_{jl} + \delta_{il}\delta_{jk}\right) \tag{A2}$$

where K and G = elastic bulk and shear moduli, which are given respectively as

$$K = \frac{E}{3(1-2\nu)} = \frac{1+e_0}{\kappa}p \tag{A3}$$

$$G = \frac{E}{2(1+\nu)} = \frac{3(1-2\nu)(1+e_0)}{2(1+\nu)\kappa}p \tag{A4}$$

Since parameters are independent of loading direction, the total differential of the yield function in Eq. (18) is still

$$\mathrm{d}f = \frac{\partial f}{\partial \sigma_{ij}}\mathrm{d}\sigma_{ij} + \frac{\partial f}{\partial \widetilde{H}}\frac{\partial \widetilde{H}}{\partial \varepsilon_{ij}^{\mathrm{p}}}\mathrm{d}\varepsilon_{ij}^{\mathrm{p}} = 0 \tag{A5}$$

The direction of plastic flow is normal to the plastic potential surface in the $\widetilde{\sigma}_{ij}$ space (see Eq. (18)) as

$$\mathrm{d}\varepsilon_{ij}^{\mathrm{p}} = \Lambda\frac{\partial g}{\partial \widetilde{\sigma}_{ij}} \tag{A6}$$

Substituting Eqs. (A1) and (A6) into Eq. (A5), the plastic factor can be obtained as

$$\Lambda = \frac{\dfrac{\partial f}{\partial \sigma_{ij}}D_{ijkl}^{\mathrm{e}}\mathrm{d}\varepsilon_{kl}}{\dfrac{\partial f}{\partial \sigma_{ij}}D_{ijkl}^{\mathrm{e}}\dfrac{\partial g}{\partial \widetilde{\sigma}_{kl}} - \dfrac{\partial f}{\partial \widetilde{H}}\dfrac{\partial \widetilde{H}}{\partial \varepsilon_{kl}^{\mathrm{p}}}\dfrac{\partial g}{\partial \widetilde{\sigma}_{kl}}} \tag{A7}$$

Then substituting Eqs. (A6) and (A7) into Eq. (A1) gives

$$\mathrm{d}\sigma_{ij} = D_{ijkl}\mathrm{d}\varepsilon_{kl} \tag{A8}$$

where D_{ijkl} = the elastoplastic constitutive tensor, which can be rewritten as

$$D_{ijkl} = D_{ijkl}^{\mathrm{e}} - \frac{D_{ijmn}^{\mathrm{e}}\dfrac{\partial g}{\partial \widetilde{\sigma}_{mn}}\dfrac{\partial f}{\partial \sigma_{st}}D_{stkl}^{\mathrm{e}}}{\dfrac{\partial f}{\partial \sigma_{ij}}D_{ijkl}^{\mathrm{e}}\dfrac{\partial g}{\partial \widetilde{\sigma}_{kl}} - \dfrac{\partial f}{\partial \widetilde{H}}\dfrac{\partial \widetilde{H}}{\partial \varepsilon_{kl}^{\mathrm{p}}}\dfrac{\partial g}{\partial \widetilde{\sigma}_{kl}}} \tag{A9}$$

where

$$\frac{\partial f}{\partial \widetilde{H}} = -\frac{1}{c_{\mathrm{p}}} \tag{A10}$$

$$\frac{\partial \widetilde{H}}{\partial \varepsilon_{ij}^{\mathrm{p}}} = \frac{\widetilde{M}_{\mathrm{f}}^{4} - \widetilde{\eta}^{4}}{\overline{M}^{4} - \widetilde{\eta}^{4}} \delta_{ij} \tag{A11}$$

$$\begin{aligned} \frac{\partial g}{\partial \widetilde{\sigma}_{ij}} &= \frac{\partial g}{\partial \widetilde{p}} \frac{\partial \widetilde{p}}{\partial \widetilde{\sigma}_{ij}} + \frac{\partial g}{\partial \widetilde{q}} \frac{\partial \widetilde{q}}{\partial \widetilde{\sigma}_{ij}} \\ &= \frac{1}{\overline{M}^{2}\widetilde{p}^{2} + \widetilde{q}^{2}} \left[\frac{\overline{M}^{2}\widetilde{p}^{2} - \widetilde{q}^{2}}{3\widetilde{p}} \delta_{ij} + 3\left(\widetilde{\sigma}_{ij} - \widetilde{p}\delta_{ij}\right) \right] \end{aligned} \tag{A12}$$

and

$$\begin{aligned} \frac{\partial f}{\partial \sigma_{ij}} &= \frac{\partial f}{\partial \overline{\sigma}_{kl}} \frac{\partial \overline{\sigma}_{kl}}{\partial \sigma_{ij}} \\ &= \frac{3}{2} \left(\frac{\partial f}{\partial \widetilde{p}} \frac{\partial \widetilde{p}}{\partial \overline{\sigma}_{kl}} + \frac{\partial f}{\partial \widetilde{q}} \frac{\partial \widetilde{q}}{\partial \overline{\sigma}_{kl}} \right) \left(F_{jl}\delta_{ki} + F_{ki}\delta_{jl} \right) \end{aligned} \tag{A13}$$

where F_{ij} should have been transformed to the physical space (Z, X, Y), and

$$\frac{\partial \widetilde{p}}{\partial \overline{\sigma}_{ij}} = \frac{\partial \overline{p}}{\partial \overline{\sigma}_{ij}} = \frac{1}{3}\delta_{ij} \tag{A14}$$

$$\frac{\partial \widetilde{q}}{\partial \overline{\sigma}_{ij}} = \frac{\partial \bar{q}_{\mathrm{c}}}{\partial \overline{\sigma}_{ij}} = \frac{\left(\bar{q}_{\mathrm{c}}^{2} - \bar{I}_{1}^{2}\right)\dfrac{\partial \bar{I}_{1}}{\partial \overline{\sigma}_{ij}} + 9\dfrac{\partial \bar{I}_{3}}{\partial \overline{\sigma}_{ij}}}{2\bar{q}_{\mathrm{c}}\left(\bar{q}_{\mathrm{c}} - \bar{I}_{1}\right)} \tag{A15}$$

Notation

b	intermediate principal stress coefficient
D_{ijkl}	elastoplastic constitutive tensor
D_{ijkl}^{e}	elastic constitutive tensor
e	void ratio
e_0	initial void ratio
F_{ij}	fabric tensor
G	elastic shear modulus
H	unified hardening parameter
$\widetilde{H}$	unified hardening parameter in the transformed stress space
I_1, I_3	first and third stress invariants, respectively
$\bar{I}_1$, $\bar{I}_3$	first and third stress invariants of the modified stress tensor, respectively
K	elastic bulk modulus
M	critical state stress ratio of triaxial compression
M_{f}	potential failure stress ratio

M_{h} failure/critical state stress ratio of HC test

M_{v} failure/critical state stress ratio of VC test

$\overline{M}$ failure/critical state stress ratio of triaxial compression in the modified stress space

$\widetilde{M}_{\mathrm{f}}$ potential failure stress ratio in the transformed stress space

p mean stress

p_{x0} intercept of the initial current yield surface on the p-axis

p' mean stress at reference stress point

p'_{x0} intercept of the initial reference yield surface on the p-axis

$\overline{p}$ mean stress of the modified stress tensor

$\widetilde{p}$ mean stress of the transformed stress tensor

$\widetilde{p}_x$ intercept of the current yield surface on the $\widetilde{p}$-axis in the transformed stress space

$\widetilde{p}_{x0}$ intercept of the initial current yield surface on the $\widetilde{p}$-axis in the transformed stress space

$\widetilde{p}'_{x0}$ intercept of the initial reference yield surface on the $\widetilde{p}$-axis in the transformed stress space

q deviatoric stress

q' deviatoric stress at reference stress point

$\overline{q}$ deviatoric stress of the modified stress tensor

$\widetilde{q}$ deviatoric stress of the transformed stress tensor

$\overline{q}_{\mathrm{c}}$ deviatoric stress at the triaxial compression state in the modified stress space

R overconsolidation parameter

$\widetilde{R}$ overconsolidation parameter in the transformed stress space

u excess pore pressure

δ angle between the Z-axis and direction of deposition

δ_{ij} Kronecker delta

Δ principal value of fabric tensor

ε_{ij} total strain tensor

$\varepsilon_{ij}^{\mathrm{e}}$ elastic strain tensor

$\varepsilon_{ij}^{\mathrm{p}}$ plastic strain tensor

$\varepsilon_{\mathrm{v}}^{\mathrm{p}}$ plastic volumetric strain

η stress ratio

$\widetilde{\eta}$ stress ratio of the transformed stress tensor

θ Lode's angle

$\overline{\theta}$ Lode's angle of the modified stress tensor

$\widetilde{\theta}$ Lode's angle of the transformed stress tensor

κ slope of swelling line

λ slope of normal compression line

ν Poisson's ratio

σ_{ij} stress tensor

$\overline{\sigma}_{ij}$ modified stress tensor

$\widetilde{\sigma}_{ij}$ transformed stress tensor

φ internal friction angle

Acknowledgements

This study is supported by the National Program on Key Basic Project of China (973 Program, Grant No. 2014CB047006), the National Natural Science Foundation of China (Grant Nos. 11272031 and 51179003).

References

1. Ladd CC. *Stress-strain behavior of anisotropically consolidated clays during undrained shear*. PhD thesis, MIT, 1964.
2. Duncan JM, Seed HB. Strength variation along failure surfaces in clay. *Journal of Soil Mechanics & Foundations Division* 1996; 92 (SM6): 81-104.
3. Arthur JR, Menzies BK. Inherent anisotropy of sand. *Géotechnique* 1972; 22(1): 115-128.
4. Arthur JR, Chua KS, Dunstan T. Induced anisotropy in a sand. *Géotechnique* 1977; 27(1): 13-30.
5. Wong RK, Arthur JR. Induced and Inherent anisotropy in sand. *Géotechnique* 1985; 35(4): 471-481.
6. Kirkgard MM, Lade PV. Anisotropic three-dimensional behavior of a normally consolidated clay. *Canadian Geotechnical Journal* 1993; 30(4): 848-858.
7. Lade PV, Abelev A. Characterization of cross-anisotropic soil deposits from isotropic compression tests. *Soils and Foundations* 2005; 45(5): 89-102.
8. Loukidis D, Salgado R. Effect of relative density and stress level on the bearing capacity of footings on sand. *Géotechnique* 2010; 61(2): 107-119.
9. Gonzalez NA, Rouainia M, Arroyo M, Gens A. Analysis of tunnel excavation in London Clay incorporating soil structure. *Géotechnique* 2012; 62(12): 1095-1109.
10. Hill R. *Mathematical theory of plasticity*, Oxford University Press, Oxford, U.K. 1950.
11. Oda M. Initial fabrics and their relations to mechanical properties of granular material. *Soils and Foundations* 1972; 12(1): 17-36.
12. Oda M, Nemat-Nasser S, Konishi J. Stress-induced anisotropy in granular masses. *Soils and Foundations* 1985; 25(3): 85-97.
13. Tobita Y. Fabric tensors in constitutive equations for granular materials. *Soils and Foundations* 1989; 29(4): 91-104.
14. Oda M, Nakayama H. Yield function for soil with anisotropic fabric. *Journal of Engineering Mechanics* 1989; 115(1): 89-104.
15. Pietruszczak S, Mroz Z. Formulation of anisotropic failure criteria incorporating a microstructure tensor. *Computers and Geotechnics* 2000; 26(2): 105-112.
16. Pietruszczak S, Mroz Z. On failure criteria for anisotropic cohesive-frictional materials. *International Journal for Numerical and Analytical Methods in Geomechanics* 2001; 25(5):

509-524.
17. Lade PV. Lade PV. Failure criterion for cross-anisotropic soils. *Journal of Geotechnical and Geoenvironmental Engineering* 2008; 134(1): 117-124.
18. Pietruszczak S, Guo P. Description of deformation process in inherently anisotropic granular materials. *International Journal for Numerical and Analytical Methods in Geomechanics* 2013; 37(5): 478-490.
19. Schweiger HF, Wiltafsky C, Scharinger F, Galavi V. A multilaminate framework for modelling induced and inherent anisotropy of soils. *Géotechnique* 2009; 59(2): 87-101.
20. Li XS, Dafalias YF. Constitutive modeling of inherently anisotropic sand behavior. *Journal of Geotechnical and Geoenvironmental Engineering* 2002; 128(10): 868-880.
21. Li XS, Dafalias YF. A constitutive framework for anisotropic sand including non-proportional loading. *Géotechnique* 2004; 54(1): 41-55.
22. Gao ZW, Zhao JD, Yao YP. A generalized anisotropic failure criterion for geomaterials. *International Journal of Solids and Structures* 2010; 47(22): 3166-3185.
23. Gao ZW, Zhao JD, Li XS, Dafalis YF. A critical state sand plasticity model accounting for fabric evolution. *International Journal for Numerical and Analytical Methods in Geomechanics* 2014; 38: 370-390.
24. Matsuoka H, Yao YP, Sun DA. The Cam-clay models revised by the SMP criterion. *Soils and Foundations* 1999; 39(1): 81-95.
25. Yao YP, Sun DA. Application of Lade's criterion to Cam-clay model. *Journal of Engineering Mechanics* 2000; 126(1): 112-119.
26. Yao YP, Wang ND. Transformed stress method for generalizing soil constitutive models. *Journal of Engineering Mechanics* 2014; 140(3): 614-629.
27. Cui L, O'sullivan C. Exploring the macro-and micro-scale response of an idealised granular material in the direct shear apparatus. *Géotechnique* 2006; 56(7): 455-468.
28. Hosseininia ES. Stress-force-fabric relationship for planar granular materials. *Géotechnique* 2013; 63(10): 830-841.
29. Li X, Yu HS, Li XS. Macro–micro relations in granular mechanics. *International Journal of Solids and Structures* 2009; 46(25): 4331-4341.
30. Yimsiri S, Soga K. Effects of soil fabric on behaviors of granular soils: Microscopic modeling. *Computers and Geotechnics* 2011; 38(7): 861-874.
31. Tobita Y. Contact tensor in constitutive model for granular materials. *Proc., U.S.-Japan seminar on micromechanics of granular materials*, Sendai-Zao, Japan, M. Satake, and J. Jenkins, eds., Elsevier, New York, 1988: 263-270.
32. Tobita Y. Modified double slip model with fabric anisotropy for hardening behavior of granular materials. *Advances in Micromechanics of Granular Materials: Proceedings of the Second US/Japan Seminar on Micromechanics of Granular Materials*, Potsdam, NY, USA, August 5-9, 1991. Elsevier, 2013: 203.

33. Saada AS, Zamani KK. The mechanical behavior of cross anisotropic clay. *Proc. 7th ICSMFE*, Mexico, 1969; 1: 351-359.
34. Saada AS. Testing of anisotropic clay soils. *Journal of the Soil Mechanics and Foundations Division* 1970; 96(5): 1847-1852.
35. Lade PV, Duncan JM. Elasto-plastic stress-strain theory for cohesionless soil. *Journal of the Geotechnical Engineering Division* 1975; 101(10): 1037-1053.
36. Matsuoka H, Nakai T. Stress-deformation and strength characteristics of soil under three different principal stresses. *Proc. JSCE* 1974; 232: 59-70.
37. Yao YP, Lu DC, Zhou AN, Zou B. Generalized non-linear strength theory and transformed stress space. *Science in China Series E: Technological Sciences* 2004; 47(6): 691-709.
38. Roscoe KH, Schofield A, Thurairajah A. Yielding of clays in states wetter than critical. *Géotechnique* 1963; 13(3): 211-240.
39. Schofield A, Wroth P. *Critical state soil mechanics*. London: McGraw-Hill, 1968.
40. Argyris JH, Faust F, Szimat J, Warnke EP, William KJ. Recent developments in the finite element analysis of prestressed concrete reactor vessels. *Nuclear Engineering and Design* 1974; 28(1): 42-75.
41. Pastor M. Modelling of anisotropic sand behaviour. *Computers and Geotechnics* 1991; 11(3): 173-208.
42. Yao YP, Hou W, Zhou AN. UH model: Three-dimensional unified hardening model for overconsolidated clays. *Géotechnique* 2009; 59(5): 451-469.
43. Yao YP, Gao ZW, Zhao JD, Wan Z. Modified UH model: constitutive modeling of overconsolidated clays based on a parabolic Hvorslev envelope. *Journal of Geotechnical and Geoenvironmental Engineering* 2012; 138(7): 860-868.
44. Sekiguchi H, Ohta H. Induced anisotropy and time dependency in clays. *Proc. 9th ICSMFE*, Tokyo, 1977: 229-238.
45. Anandarajah A, Dafalias YF. Bounding surface plasticity. III: application to anisotropic cohesive soils. *Journal of Engineering Mechanics* 1986; 112(12): 1292-1318.
46. El-Sohby MA, Andrawes KZ. Experimental examination of sand anisotropy. *Proc. 8th ICSMFE*, Moscow, 1973: 6-11.
47. Abelev A, Lade PV. Characterization of failure in cross-anisotropic soils. *Journal of Engineering Mechanics* 2004; 130(5): 599-606.
48. Mitchell RJ. Some deviations from isotropy in a lightly overconsolidated clay. *Géotechnique* 1972; 22(3): 459-467.
49. Banerjee PK, Yousif NB. A plasticity model for the mechanical behavior of anisotropically consolidated clay. *International Journal for Numerical and Analytical Methods in Geomechanics* 1986; 10: 521-541.
50. Stipho AS. *Experimental and theoretical investigation of the behavior of anisotropically consolidated Kaolin*. PhD thesis. Univ. College, Cardiff, U.K. 1978.